Journal of Solid Mechanics Vol. 9, No. 1 (2017) pp. 100-114

Stress Analysis of Rotating Thick Truncated Conical Shells with Variable Thickness under Mechanical and Thermal Loads

M. Jabbari [1], M. Zamani Nejad [1,*],M. Ghannad [2]

[1]*Mechanical Engineering Department, Yasouj University, P.O.Box: 75914-353, Yasouj, Iran*
[2]*Mechanical Engineering Faculty, Shahrood University, Shahrood, Iran*

Received 3 November 2016; accepted 2 January 2017

ABSTRACT

In this paper, thermo-elastic analysis of a rotating thick truncated conical shell subjected to the temperature gradient, internal pressure and external pressure is presented. Given the existence of shear stress in the conical shell due to thickness change along the axial direction, the governing equations are obtained based on first-order shear deformation theory (FSDT). These equations are solved by using multi-layer method (MLM). The model has been verified with the results of finite element method (FEM). Finally, some numerical results are presented to study the effects of thermal and mechanical loading, geometry parameters of truncated conical shell.

Keywords : Pressurized conical shells; Variable thickness; Thermo-elastic analysis; Rotation; Multi-layer method (MLM).

1 INTRODUCTION

THICK conical shells are increasingly being put to numerous engineering applications such as hoppers, vessel heads, components of missiles and spacecraft, heart ventricles, diffusers and other civil, mechanical and aerospace engineering structures [1]. Since in most applications, conical shells must operate under extremes of thermal and mechanical loadings, any failure or fracture will be an irreparable disaster. So, adequate strength consideration is so important for these components [2-4].

From early thermo-elastic analyses on conical shells, Witt [5] derived a differential equation of a conical shell subjected to axis-symmetrical temperature distributions. In order to obtain a particular solution to the differential equation, he assumed the expression for the temperature distributions to be the sum of hyperbolic and cubic functions. Panferov [6] used the method of successive approximations to obtain the solution of the problem of thermal loading of an elastic truncated conical pipe with constant thickness. Sundarasivarao and Ganesan [7] analyzed a conical shell under pressure using the finite element method. A generalized thermoelasticity problem of multilayered conical shells was presented in Jane and Wu [8]. Vivio and Vullo [9] presented an analytical procedure for the evaluation of elastic stresses and strains in rotating conical disks, either solid or annular, subjected to thermal load, with a fictitious density variation along the radius. Naj et al. [10] studied thermal and mechanical instability of truncated conical shells made of functionally graded materials.

For elastic analysis a thick conical shell with varying thickness under nonuniform internal pressure, Eipakchi et al. [11] used the mathematical approach based on the perturbation theory. Saldek et al. [12] solved problems of

*Corresponding author. Tel.: +98 74 33221711; Fax: +98 74 33221711.
E-mail address: m_zamani@yu.ac.ir (M. Zamani Nejad).

Reissner-Mindlin shells under thermal loading. Using the tensor analysis, Nejad et al. [13] obtained a complete and consistent 3-D set of field equations to characterize the behavior of functionally graded material thick shells of revolution with arbitrary curvature and variable thickness. Based on first-order shear deformation theory (FSDT) and the virtual work principle, Ghannad et al. [14], obtained an elastic solution for thick truncated conical shells with constant thickness. Eipakchi [15] calculated displacements and stresses of a thick conical shell with varying thickness subjected to non-uniform internal pressure using a third-order shear deformation theory for the homogeneous, isotropic, and axisymmetric cases by using the matched asymptotic expansion of perturbation theory. He concluded that FSDT is sufficient for the purpose of determining displacements. Jabbari et al. [16] presented the general solution of steady-state two-dimensional non-axisymmetric mechanical and thermal stresses and mechanical displacements of a hollow thick cylinder made of fluid-saturated functionally graded porous material. Ray et al. [17] carried out an analysis of conduction heat transfer through conical shells of different inner radii and shell thicknesses. Based on the high-order shear deformation theory, Ghannad and Gharooni [18] presented displacements and stresses for axisymmetric thick-walled cylinders made of functionally graded materials under internal and/or external uniform pressure by using the infinitesimal theory of elasticity and analytical formulation.

More recently, based on FSDT and the virtual work principle, Ghannad et al. [19] performed an elastic analysis for axisymmetric clamped-clamped pressurized thick truncated conical shells with constant thickness made of radially functionally graded materials. Nejad et al. [20] derived an elastic solution for the purpose of determining displacements and stresses in a thick truncated conical shell under uniform pressure where multi-layer method (MLM) has been used for solution. They also used this method to the analysis of a rotating truncated conical shell [21]. Jabbari and Meshkini [22] developed the general solution of steady state on one-dimensional axisymmetric mechanical and thermal stresses for a hollow thick made of cylinder functionally graded porous material. Making use of FSDT and MLM, Nejad et al. [23] performed a semi-analytical solution for the purpose of elastic analysis of rotating thick truncated conical shells made of functionally graded material under non-uniform pressure. Sofiyev et al. [24] presented analytical formulations and solutions for the stability analysis of heterogeneous orthotropic truncated conical shell subjected to external (lateral and hydrostatic) pressures with mixed boundary conditions using the Donnell shell theory. Jabbari et al. [25] carried out a study of thermoelastic analysis of a rotating thick truncated conical shell with constant thickness subjected to the temperature gradient and non-uniform internal pressure .

In this work, a thermo-elastic analysis of a pressurized thick truncated conical shell with variable thickness is presented. The governing equations are based on FSDT that accounts for the transverse shear. The governing equations are derived, using minimum total potential energy principle. The heat conduction is also taken into consideration in the analysis. These equations in the axisymmetric case and thermo-elasto-static state constitute a system of ordinary differential equations with variable coefficients. Normally, these equations do not have exact solutions. The MLM is used in order to solve the system of equations with variable coefficients. For this purpose, a rotating conical shell with variable thickness is divided into disks with constant thickness. With regard to the continuity between layers and applying boundary conditions, the governing set of differential equations with constant coefficients is solved. The results are compared with those derived through the finite element method (FEM) for some load cases. By numerically solving the resulting equations, the distribution of the thermal stress and displacement components can be obtained and the numerical results of the thermal stresses are presented graphically to show the effect of loading parameters on the distribution of thermal stresses and displacements. Finally, the conclusions drawn from the present study are reported.

2 GOVERNING EQUATION

Geometry and boundary condition and loading condition of a thick conical shell with variable thickness h, and the length L, are shown in Fig.1.

The location of any typical point on the longitudinal section of an axisymmetric conical shell can be defined by two parameters r and x, where x is the axial coordinate and r is the radius, which is perpendicular to x and satisfies $r = R + z$; R is the middle surface radius, and z is a trough thickness variable, which is measured from the middle surface (Fig.1).

$$R = R_1 + \frac{h}{2} + \left(\frac{R_2 - R_1}{L} \right) x \tag{1}$$

where

$$h = h_1 + \left(\frac{h_2 - h_1}{L}\right)x \tag{2}$$

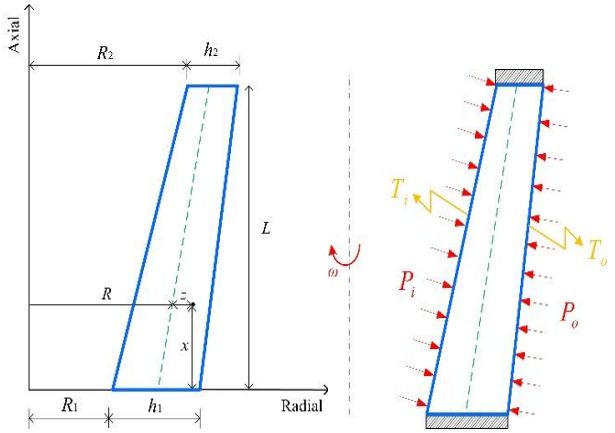

Fig.1
Cross-section of the clamped-clamped thick rotating cone with variable thickness.

The general axisymmetric displacement field (U_x, U_z), in the FSDT could be expressed on the basis of axial and radial displacements, as follows:

$$U_x = u_0(x) + zu_1(x), U_\theta = 0, U_z = w_0(x) + zw_1(x) \tag{3}$$

where $u(x)$ and $w(x)$ are the displacement components of the middle surface. Also, $\phi(x)$ and $\psi(x)$ are the functions of displacement field. The strain-displacement relations in the cylindrical coordinates system are.

$$\varepsilon_x = \frac{\partial U_x}{\partial x}, \varepsilon_\theta = \frac{U_z}{r}, \varepsilon_z = \frac{\partial U_z}{\partial z}, \gamma_{xz} = \frac{\partial U_x}{\partial z} + \frac{\partial U_z}{\partial x} \tag{4}$$

Considering the effect of the thermal strain for homogeneous and isotropic materials, the stress-strain relations (i.e., constitutive equations) are as follows:

$$\begin{aligned} \sigma_i &= \frac{E}{(1+\nu)(1-2\nu)}\left[(1-\nu)\varepsilon_i + \nu(\varepsilon_j + \varepsilon_k)\right] - \frac{E}{(1-2\nu)}\alpha T \quad , \quad i \neq j \neq k \\ \tau_{xz} &= \frac{E}{2(1+\nu)}\gamma_{xz} \end{aligned} \tag{5}$$

where σ_i and ε_i are the stresses and strains. E, T, α and ν are the modulus of elasticity, temperature gradient, thermal expansion coefficient and Poisson's ratio respectively. The stress resultants are defined as:

$$\begin{Bmatrix} N_x \\ M_x \end{Bmatrix} = \int_{-h/2}^{h/2} \begin{Bmatrix} 1 \\ z \end{Bmatrix} \frac{\sigma_x}{R}(z+R)\,dz \tag{6}$$

$$\begin{Bmatrix} N_\theta \\ M_\theta \end{Bmatrix} = \int_{-h/2}^{h/2} \begin{Bmatrix} 1 \\ z \end{Bmatrix} \sigma_\theta\,dz \tag{7}$$

$$\begin{Bmatrix} N_z \\ M_z \end{Bmatrix} = \int_{-h/2}^{h/2} \begin{Bmatrix} 1 \\ z \end{Bmatrix} \frac{\sigma_z}{R}(z+R)\,dz \tag{8}$$

$$\begin{Bmatrix} Q_x \\ M_{xz} \end{Bmatrix} = K \int_{-h/2}^{h/2} \begin{Bmatrix} 1 \\ z \end{Bmatrix} \frac{\tau_{xz}}{R}(z+R)\,dz \tag{9}$$

where K is the shear correction factor that is embedded in the shear stress term. In the static state, for conical shells $K = 5/6$ [26]. The governing equations can be derived using the principle of virtual work, which states that $\delta U = \delta W$, where δU is the total strain energy of the elastic body and δW is the total external work. The variations of the strain energy and variation of the external work are

$$\delta U = \int_0^{2\pi}\int_0^{L}\int_{-h/2}^{h/2} (\sigma_x \delta\varepsilon_x + \sigma_\theta \delta\varepsilon_\theta + \sigma_z \delta\varepsilon_z + \tau_{xz}\delta\gamma_{xz})(R+z)\,dz dx d\theta \tag{10}$$

$$\delta W = -\int_0^{2\pi}\int_0^{L} \left(P_{iz}\delta U_z + P_{ix}\delta U_x\right)\left(R - \frac{h}{2}\right) dx\,d\theta + \int_0^{2\pi}\int_0^{L} \left(P_{oz}\delta U_z + P_{ox}\delta U_x\right)\left(R + \frac{h}{2}\right) dx\,d\theta \tag{11}$$

where ρ is the density of truncated conical shell. Applied pressure to internal and external surface derived as follows:

$$P_{ix} = \frac{|R_1 - R_2| P_i}{\sqrt{L^2 + (R_1 - R_2)^2}}, P_{iz} = \frac{L P_i}{\sqrt{L^2 + (R_1 - R_2)^2}} \tag{12}$$

$$P_{ox} = \frac{|R_1 + h_1 - R_2 - h_2| P_o}{\sqrt{L^2 + (R_1 + h_1 - R_2 - h_2)^2}}, P_{oz} = \frac{L P_o}{\sqrt{L^2 + (R_1 + h_1 - R_2 - h_2)^2}}, \tag{13}$$

Substituting Eqs. (10) and (11) into $\delta U = \delta W$, and drawing upon the calculus of variation and the virtual work principle, we will have:

$$(1-\nu)\frac{h^3}{12}\frac{du_1}{dx} + (1-\nu)Rh\frac{du_0}{dx} + \nu h w_0 + \nu R h w_1 = F_1 \tag{14}$$

$$\begin{aligned}&(1-\nu)\frac{h^3}{12}\left(\frac{d^2u_0}{dx^2} + R\frac{d^2u_1}{dx^2} + \left(h\frac{dR}{dx} + 3R\frac{dh}{dx}\right)\frac{du_1}{dx} + 3\frac{dh}{dx}\frac{du_0}{dx}\right) - \frac{(\mu - 2\nu)h^3}{12}\frac{dw_1}{dx} - \mu Rh\left(\frac{dw_0}{dx} + u_1\right) \\ &+\nu\frac{h^2}{6}\frac{dh}{dx}w_1 = F_2\end{aligned} \tag{15}$$

$$\begin{aligned}&\mu Rh\left(\frac{d^2w_0}{dx^2} + \frac{du_1}{dx}\right) + \frac{\mu h^2}{12}\left(h\frac{d^2w_1}{dx^2} + 3\frac{dh}{dx}\frac{dw_1}{dx}\right) + \mu h\frac{d}{dx}(Rh)\left(\frac{dw_0}{dx} + u_1\right) - (1-\nu)xw_0 \\ &+\left((1-\nu)Rx - h\right)w_1 - \nu h\frac{du_0}{dx} = F_3\end{aligned} \tag{16}$$

$$\frac{\mu h^3}{12}\left(\frac{d^2w_0}{dx^2}+R\frac{d^2w_1}{dx^2}\right)+\frac{(\mu-2\nu)h^3}{12}\frac{du_1}{dx}+\mu\frac{h^2}{12}\left(3\left(\frac{dw_0}{dx}+u_1\right)\frac{dh}{dx}+\left(h\frac{dR}{dx}+3R\frac{dh}{dx}\right)\frac{dw_1}{dx}\right)$$
$$-\nu Rh\frac{du_0}{dx}-(1-\nu)R^2xw_1+\left((1-\nu)Rx-h\right)w_0=F_4 \tag{17}$$

where

$$\mu=\frac{5}{12}(1-2\nu),x=\ln\left(\frac{R+h/2}{R-h/2}\right) \tag{18}$$

$$\begin{cases}F_1=C_0+\alpha(1-2\nu)\int_{-h/2}^{h/2}(R+z)Tdz-\dfrac{(1+\nu)(1-2\nu)}{E}\int\left(P_{ix}\left(R-\dfrac{h}{2}\right)-P_{ox}\left(R+\dfrac{h}{2}\right)\right)dx\\ F_2=\dfrac{(1+\nu)(1-2\nu)}{E}\dfrac{h}{2}\left(P_{ix}\left(R-\dfrac{h}{2}\right)+P_{ox}\left(R+\dfrac{h}{2}\right)\right)\\ F_3=\alpha(1-2\nu)\int_{-h/2}^{h/2}Tdz-\dfrac{(1+\nu)(1-2\nu)}{E}\left(P_{iz}\left(R-\dfrac{h}{2}\right)-P_{oz}\left(R+\dfrac{h}{2}\right)+\dfrac{\rho\omega^2h}{12}\left(12R^2+h^2\right)\right)\\ F_4=\alpha(1-2\nu)\int_{-h/2}^{h/2}(R+2z)Tdz+\dfrac{(1+\nu)(1-2\nu)}{E}\dfrac{h}{2}\left(\left(P_{iz}\left(R-\dfrac{h}{2}\right)+P_{oz}\left(R+\dfrac{h}{2}\right)\right)-\dfrac{\rho\omega^2}{3}Rh^2\right)\end{cases} \tag{19}$$

Considering the terms of internal and external pressures, rotation and thermal gradient which have been revealed in the non-homogeneity of the set of governing differential equations, the superposition principle could be utilized. It means that for rotating pressurized conical shell under thermal gradient, it would be possible to consider the effect of each loading and finally on the basis of superposition method, add the displacements and stresses resulted from individual loading.

3 SEMI-ANALYTICAL SOLUTION

3.1 Multi-layered formulation

Eqs. (14)-(17) are the set of non-homogenous linear differential equations with variable coefficients. An analytical solution of this set of differential equations with variable coefficients seems to be difficult, if not impossible, to obtain. Hence, in the current study, MLM for the solution of the set of non-homogenous linear differential equations is presented. In MLM, a cone with variable thickness is divided into n_d disk layers with constant thickness $h^{[k]}$ (Fig. 2).

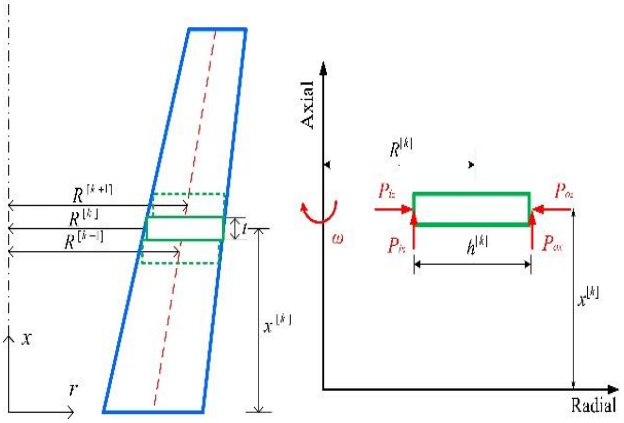

Fig.2
Geometry of an arbitrary homogenous disk layer.

Therefore, the governing equations convert to a nonhomogeneous set of differential equations with constant coefficients. The radius of the middle point of each disk is as follows:

$$R^{[k]} = R_1 + \frac{h^{[k]}}{2} + \left(\frac{R_2 - R_1}{L}\right) x^{[k]} \tag{20}$$

where

$$h^{[k]} = h_1 + \left(\frac{h_2 - h_1}{L}\right) x^{[k]} \tag{21}$$

$$x^{[k]} = \frac{L}{n_d}\left(k - \frac{1}{2}\right) \tag{22}$$

K is the corresponding number given to each disk. Thus

$$\left(\frac{dR}{dx}\right)^{[k]} = \frac{R_2 - R_1}{L} \tag{23}$$

$$\left(\frac{dh}{dx}\right)^{[k]} = \frac{h_2 - h_1}{L} \tag{24}$$

with regard to shear stress and based on FSDT, a nonhomogeneous set of differential equations with constant coefficient is obtained for each homogenous disk

$$\frac{(1-\nu)\left(h^{[k]}\right)^3}{12}\frac{du_1^{[k]}}{dx} + (1-\nu)R^{[k]}h^{[k]}\frac{du_0^{[k]}}{dx} + \nu h^{[k]}w_0^{[k]} + \nu R^{[k]}h^{[k]}w_1^{[k]} = F_1^{[k]} \tag{25}$$

$$\begin{aligned}&\frac{(1-\nu)\left(h^{[k]}\right)^3}{12}\left(\frac{d^2u_0^{[k]}}{dx^2} + R^{[k]}\frac{d^2u_1^{[k]}}{dx^2} + \left(h^{[k]}\left(\frac{dR}{dx}\right)^{[k]} + 3R^{[k]}\left(\frac{dh}{dx}\right)^{[k]}\right)\frac{du_1^{[k]}}{dx} + 3\left(\frac{dh}{dx}\right)^{[k]}\frac{du_0^{[k]}}{dx}\right)\\ &-\mu R^{[k]}h^{[k]}\left(u_1^{[k]} + \frac{dw_0^{[k]}}{dx}\right) - \frac{(\mu-2\nu)\left(h^{[k]}\right)^3}{12}\frac{dw_1^{[k]}}{dx} + \frac{\nu\left(h^{[k]}\right)^2}{2}\left(\frac{dh}{dx}\right)^{[k]}w_1^{[k]} = F_2^{[k]}\end{aligned} \tag{26}$$

$$\begin{aligned}&\mu R^{[k]}h^{[k]}\left(\frac{d^2w_0^{[k]}}{dx^2} + \frac{du_1^{[k]}}{dx}\right) + \frac{\mu^{[k]}\left(h^{[k]}\right)^2}{12}\left(h^{[k]}\frac{d^2w_1^{[k]}}{dx^2} + 3\left(\frac{dh}{dx}\right)^{[k]}\frac{dw_1^{[k]}}{dx}\right) + h^{[k]}w_1^{[k]} - \nu h^{[k]}\frac{du_0^{[k]}}{dx}\\ &+\mu h^{[k]}\left(h^{[k]}\left(\frac{dR}{dx}\right)^{[k]} + R^{[k]}\left(\frac{dh}{dx}\right)^{[k]}\right)\left(\frac{dw_0^{[k]}}{dx} + u_1^{[k]}\right) - (1-\nu)\chi^{[k]}\left(w_0^{[k]} - R^{[k]}w_1^{[k]}\right) = F_3^{[k]}\end{aligned} \tag{27}$$

$$\begin{aligned}&\frac{\mu\left(h^{[k]}\right)^3}{12}\left(\frac{d^2w_0^{[k]}}{dx^2} + R^{[k]}\frac{d^2w_1^{[k]}}{dx^2}\right) + \frac{(\mu-2\nu)\left(h^{[k]}\right)^3}{12}\frac{du_1^{[k]}}{dx} + \left((1-\nu)R^{[k]}\chi^{[k]}\right)\left(w_0^{[k]} - R^{[k]}w_1^{[k]}\right) - h^{[k]}w_0^{[k]}\\ &+\mu\frac{\left(h^{[k]}\right)^2}{12}\left(\left(h^{[k]}\left(\frac{dR}{dx}\right)^{[k]} + 3R^{[k]}\left(\frac{dh}{dx}\right)^{[k]}\right)\frac{dw_1^{[k]}}{dx} + 3\left(\frac{dh}{dx}\right)^{[k]}\left(\frac{dw_0^{[k]}}{dx} + u_1^{[k]}\right)\right) - \nu R^{[k]}h^{[k]}\frac{du_0^{[k]}}{dx} = F_4^{[k]}\end{aligned} \tag{28}$$

where

$$x^{[k]} = \ln\left(\frac{R^{[k]} + \frac{h^{[k]}}{2}}{R^{[k]} - \frac{h^{[k]}}{2}}\right) \tag{29}$$

$$\begin{cases} F_1^{[k]} = C_0^{[k]} + \alpha(1-2\nu)\int_{-h^{[k]}/2}^{h^{[k]}/2}\left(R^{[k]}+z\right)T^{[k]}dz - \frac{(1+\nu)(1-2\nu)}{E}\int\left(P_{ix}\left(R^{[k]}-\frac{h^{[k]}}{2}\right)-P_{ox}\left(R^{[k]}+\frac{h^{[k]}}{2}\right)\right)dx \\ F_2^{[k]} = \frac{(1+\nu)(1-2\nu)}{E}\frac{h^{[k]}}{2}\left(P_{ix}\left(R^{[k]}-\frac{h^{[k]}}{2}\right)+P_{ox}\left(R^{[k]}+\frac{h^{[k]}}{2}\right)\right) \\ F_3^{[k]} = \alpha(1-2\nu)\int_{-h^{[k]}/2}^{h^{[k]}/2}T^{[k]}dz - \frac{(1+\nu)(1-2\nu)}{E}\left(P_{iz}\left(R^{[k]}-\frac{h^{[k]}}{2}\right)-P_{oz}\left(R^{[k]}+\frac{h^{[k]}}{2}\right)+\frac{\rho\omega^2 h^{[k]}}{12}\left(12\left(R^{[k]}\right)^2+\left(h^{[k]}\right)^2\right)\right) \\ F_4^{[k]} = \alpha(1-2\nu)\int_{-h^{[k]}/2}^{h^{[k]}/2}\left(R^{[k]}+2z\right)T^{[k]}dz + \frac{(1+\nu)(1-2\nu)}{E}\frac{h^{[k]}}{2}\left(\left(P_{iz}\left(R^{[k]}-\frac{h^{[k]}}{2}\right)+P_{oz}\left(R^{[k]}+\frac{h^{[k]}}{2}\right)\right)-\frac{\rho\omega^2 R^{[k]}\left(h^{[k]}\right)^2}{3}\right) \end{cases} \tag{30}$$

3.2 Heat conduction equation

In the general form, the temperature distribution is the function of the axial and radial direction of the truncated cone. By dividing the truncated cone into disk form multilayer, the variation of temperature is assumed to occur in the radius direction only. By assumption of an element in the cylindrical coordinate system in the steady state without internal heat source, according to the heat balance equation for steady-state heat conduction without heat generation, Eq. (31) for each disk has been conducted

$$\frac{d}{dz}\left(\kappa\left(R^{[k]}+z\right)\frac{dT}{dz}\right)=0 \tag{31}$$

Solving the differential Eq. (31) the terms of temperature gradient are derived as follows:

$$T^{[k]} = d_1^{[k]}\int_{-h^{[k]}/2}^{h^{[k]}/2}\frac{dz}{\kappa\left(R^{[k]}+z\right)} + d_2^{[k]} - T_{ref} \tag{32}$$

where $d_1^{[k]}$ and $d_2^{[k]}$ are constants of integration and T_{ref} is the reference temperature. The thermal boundary conditions are expressed as (see Fig. 1)

$$\begin{cases} T^{[k]}\big|_{z=-h^{[k]}/2} = T_i \\ T^{[k]}\big|_{z=h^{[k]}/2} = T_o \end{cases} \tag{33}$$

If the $T_o = T_{ref}$, temperature gradient distribution is obtained as:

$$T^{[k]} = \left(T_o - T_i\right)\left(\frac{\ln\left(\frac{R^{[k]}+z}{R^{[k]}-h^{[k]}/2}\right)}{\ln\left(\frac{R^{[k]}+h^{[k]}/2}{R^{[k]}-h^{[k]}/2}\right)}-1\right) \tag{34}$$

3.3 Thermo-elastic solution

According to Eq. (34) and by defining the differential operator $P(D)$, Eqs. (25)-(28) are written as:

$$[P(D)]\left\{\frac{du_0^{[k]}}{dx} \quad u_1^{[k]} \quad w_0^{[k]} \quad w_1^{[k]}\right\}^T = \left\{F^{[k]}\right\} \tag{35}$$

The differential equations given above have the total solution including the general solution for the homogeneous case and the particular solution, as follows:

$$\begin{Bmatrix} U_x^{[k]} \\ U_z^{[k]} \end{Bmatrix} = \begin{Bmatrix} u_0^{[k]} + zu_1^{[k]} \\ w_0^{[k]} + zw_1^{[k]} \end{Bmatrix} \tag{36}$$

where

$$u_0^{[k]} = \int \frac{du_0^{[k]}}{dx} dx + C_7^{[k]} \tag{37}$$

For the homogeneous case, the homogeneous solution is

$$\begin{Bmatrix} U_x^{[k]} \\ U_z^{[k]} \end{Bmatrix}_h = \sum_{i=1}^{6} C_i^{[k]} \{V\}_i^{[k]} e^{m_i^{[k]} x} \tag{38}$$

The particular solution is obtained by solving follow equations

$$(1-\nu) R^{[k]} h^{[k]} \left\{\frac{du_0^{[k]}}{dx}\right\}_p + \nu h^{[k]} \left\{w_0^{[k]}\right\}_p + \nu R^{[k]} h^{[k]} \left\{w_1^{[k]}\right\}_p = F_1^{[k]} \tag{39}$$

$$+\nu \frac{\left(h^{[k]}\right)^2}{2} \left(\frac{dh}{dx}\right)^{[k]} \left\{w_1^{[k]}\right\}_p + (1-\nu) \frac{\left(h^{[k]}\right)^2}{4} \left(\frac{dh}{dx}\right)^{[k]} \left\{\frac{du_0^{[k]}}{dx}\right\}_p - \mu R^{[k]} h^{[k]} \left\{u_1^{[k]}\right\}_p = F_2^{[k]} \tag{40}$$

$$\begin{aligned} &\mu h^{[k]} \left(h^{[k]} \left(\frac{dR}{dx}\right)^{[k]} + R^{[k]} \left(\frac{dh}{dx}\right)^{[k]} \right) \left\{u_1^{[k]}\right\}_p + h^{[k]} \left(\left\{w_1^{[k]}\right\}_p - \nu \left\{\frac{du_0^{[k]}}{dx}\right\}_p \right) \\ &-(1-\nu) x^{[k]} \left(\left\{w_0^{[k]}\right\}_p - R^{[k]} \left\{w_1^{[k]}\right\}_p \right) = F_3^{[k]} \end{aligned} \tag{41}$$

$$\mu \frac{\left(h^{[k]}\right)^2}{4} \left(\frac{dh}{dx}\right)^{[k]} \left\{u_1^{[k]}\right\}_p - \nu R^{[k]} h^{[k]} \left\{\frac{du_0^{[k]}}{dx}\right\}_p + (1-\nu) x^{[k]} \left(\left\{w_0^{[k]}\right\}_p - R^{[k]} \left\{w_1^{[k]}\right\}_p \right) - h^{[k]} \left\{w_0^{[k]}\right\}_p = F_4^{[k]} \tag{42}$$

which

$$\begin{Bmatrix} U_x^{[k]} \\ U_z^{[k]} \end{Bmatrix}_p = \begin{Bmatrix} \left\{u_0^{[k]}\right\}_p + z \left\{u_1^{[k]}\right\}_p \\ \left\{w_0^{[k]}\right\}_p + z \left\{w_1^{[k]}\right\}_p \end{Bmatrix} \tag{43}$$

Therefore, the total solution is

$$\begin{Bmatrix} U_x^{[k]} \\ U_z^{[k]} \end{Bmatrix} = \begin{Bmatrix} U_x^{[k]} \\ U_z^{[k]} \end{Bmatrix}_h + \begin{Bmatrix} U_x^{[k]} \\ U_z^{[k]} \end{Bmatrix}_p \tag{44}$$

In general, the problem for each disk consists of 8 unknown values of $C_i^{[k]}$. The thermo-elastic solution is completed by the application of the boundary and continuity conditions.

3.4 Boundary and continuity conditions

Using SDT, it could be assumed that the cone has boundary conditions other than free–free ends. The clamped–clamped (fixed–fixed) boundary is straightforward and implies that the ends of the cone are restrained in all coordinate directions and even with that the plane along the edge of the cross-section is assumed not to rotate as opposed to a line tangent to the mid-surface of the shell as in thin shell theories. Simple support end conditions can be given a variety of interpretations. Classically, a simple support boundary condition is characterized with a hinge (ball and socket in three dimensions) or roller if motion is not restrained in all directions [27]. In Table 1. the details of boundary condition for the rotating truncated conical shell are presented.

Table 1
Boundary conditions for each end of truncated cone.

Clamped supported	Simply supported	Free end
$u_0 = 0$	$u_0 = 0$	$N_x = 0$
$u_1 = 0$	$M_x = 0$	$M_x = 0$
$w_0 = 0$	$w_0 = 0$	$Q_x = 0$
$w_1 = 0$	$M_{xz} = 0$	$M_{xz} = 0$

In this work, two end edges of the conical shells are assumed to be clamped supported. Because of continuity and homogeneity of the truncated cone, at the boundary between the two layers, forces, stresses and displacements must be continuous. Given that shear deformation theory applied is an approximation of one order and also all equations related to the stresses include the first derivatives of displacement, the continuity conditions are as follows:

$$\begin{Bmatrix} U_x^{[k-1]}(x,z) \\ U_z^{[k-1]}(x,z) \end{Bmatrix}_{x=x^{[k-1]}+\frac{t}{2}} = \begin{Bmatrix} U_x^{[k]}(x,z) \\ U_z^{[k]}(x,z) \end{Bmatrix}_{x=x^{[k]}-\frac{t}{2}} \tag{45}$$

$$\begin{Bmatrix} U_x^{[k]}(x,z) \\ U_z^{[k]}(x,z) \end{Bmatrix}_{x=x^{[k]}+\frac{t}{2}} = \begin{Bmatrix} U_x^{[k+1]}(x,z) \\ U_z^{[k+1]}(x,z) \end{Bmatrix}_{x=x^{[k+1]}-\frac{t}{2}} \tag{46}$$

And

$$\begin{Bmatrix} \frac{dU_x^{[k-1]}(x,z)}{dx} \\ \frac{dU_z^{[k-1]}(x,z)}{dx} \end{Bmatrix}_{x=x^{[k-1]}+\frac{t}{2}} = \begin{Bmatrix} \frac{dU_x^{[k]}(x,z)}{dx} \\ \frac{dU_z^{[k]}(x,z)}{dx} \end{Bmatrix}_{x=x^{[k]}-\frac{t}{2}} \tag{47}$$

$$\left\{\begin{matrix}\dfrac{dU_x^{[k]}(x,z)}{dx}\\ \dfrac{dU_z^{[k]}(x,z)}{dx}\end{matrix}\right\}_{x=x^{[k]}+\frac{t}{2}}=\left\{\begin{matrix}\dfrac{dU_x^{[k+1]}(x,z)}{dx}\\ \dfrac{dU_z^{[k+1]}(x,z)}{dx}\end{matrix}\right\}_{x=x^{[k+1]}-\frac{t}{2}} \tag{48}$$

Given the continuity conditions, in terms of z , 8 equations are obtained. In general, if the truncated cone is divided into n disk layers, $8(n_d-1)$ equations are obtained. Using the 8 equations of the boundary condition, $8n_d$ equations are obtained. The solution of these equations yields $8n_d$ unknown constants ($C_i, i=0.7$).

4 RESULTS AND DISCUSSION

In order to compute the numerical results, a homogeneous and isotropic truncated conical shell with $R_1=40mm$, $R_2=60mm$, $h_1=20mm$, $h_2=30mm$ and $L=400mm$ will be considered. The Young's Modulus, Poisson's ratio, thermal expansion coefficient and thermal conductivity respectively, have values of $E=70\,GPa$, $\nu=0.3$, $\alpha=24\times10^{-6}1/℃$ and $\kappa=205W/m^{\circ}C$. The internal pressure applied is $P_i=40MPa$ and external pressure is $P_o=20MPa$ respectively. The truncated cone rotates with $\omega=1000\,rad/s$ and has clamped-clamped boundary conditions. The boundary conditions for temperature are taken as $T_i=100^{\circ}C$ and $T_o=25^{\circ}C$. The results are presented in a non-dimensional form. Displacement and stresses are normalized by dividing to the internal radii and internal pressure respectively. In the problem in question 60 disks are used [17]. Firstly, the results for the radial displacement and stresses of conical shell with clamped-clamped boundary conditions are compared with those of finite element solution in Figs. 3-6. It can be seen that this solution is in good agreement with verified FEM results. The distribution of radial displacement at different layers is plotted in Fig. 3. The radial displacement at points away from the boundaries depends on radius and length. According to Fig. 3 the change in radial displacements in the lower boundary is greater than that of the upper boundary. Distribution of circumferential stress in different layers is shown in Fig. 4. It can be observed that the circumferential stress at layers close to the external surface is positive (tensile) and at other layers negative (compressive). Fig. 5 displays the radial stress distribution of isotropic truncated conical shells in different layers. As seen, the greatest radial stress occurs in the boundary layers (in this case: internal surface due to $P_i>P_o$). Fig. 6 shows the distribution of von Mises stress at different layers. It can be noted that at points near the boundaries, the von Mises stress is significant, especially in the internal surface, which is the greatest.

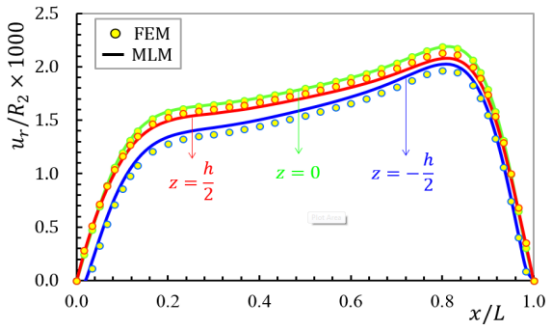

Fig.3
Normalized radial displacement distribution in different layers.

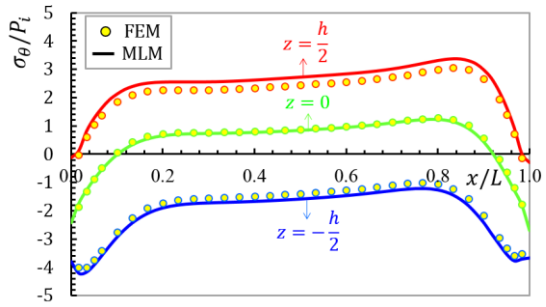

Fig.4
Normalized circumferential displacement distribution in different layers.

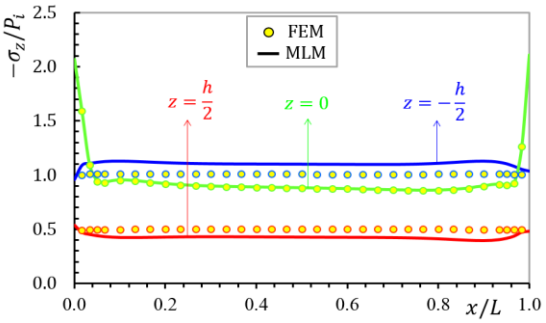

Fig.5
Normalized radial stress distribution in different layers.

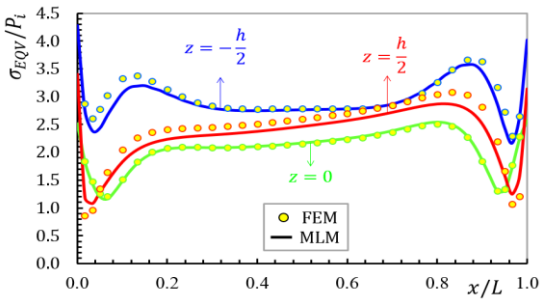

Fig.6
Normalized von Mises stress distribution in different layers.

To clarify the effect of inner radii on the mechanical behaviour of the conical shell, the non-dimensional radial displacement distribution on the axial direction is illustrated in Fig. 7. The greater the inner radii, the greater the radial displacement. The greatest radial displacement occurs in the upper boundary for $R_1/R_2>1$. In a like manner, the distribution of the von Mises stress in the middle surface is illustrated in Fig. 8. It is noticed that von Mises stress at points near the lower boundary rises as R_1/R_2 increases. But at points near the upper boundary, the situation is reverse, i.e. the von Mises stress decreases as R_1/R_2 increases.

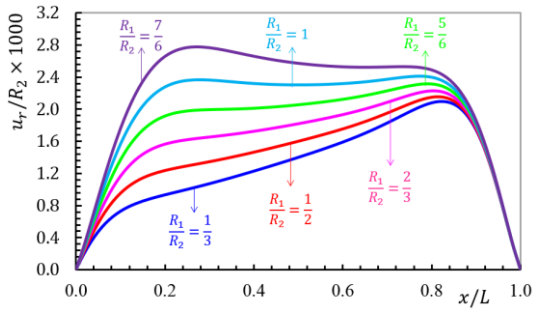

Fig.7
Distribution of non-dimensional radial displacement for different values of R_1 in the middle surface.

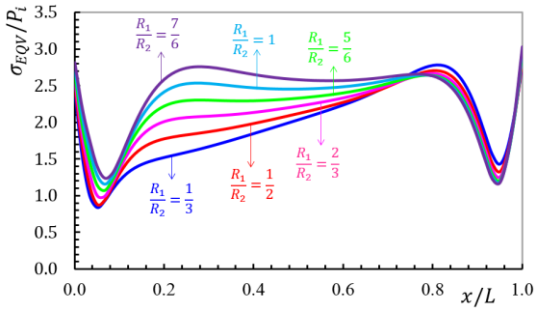

Fig.8
Distribution of non-dimensional von Mises stress for different values of R_1 in the middle surface.

The influence of the shell thickness on the radial displacement and von Mises stress are presented in Figs. 9 and 10. It can be seen that the cone with lower thickness has higher equivalent stress and radial displacement compared to cone with higher thickness. Furthermore, cones with variable thickness ($h_1 / h_2 > 1$) given have smaller equivalent stresses and radial displacement compared to uniform thickness cone. As expected the cone with constant thickness turns out to be better than those with $h_1 / h_2 < 1$. Moreover, for the thickness ratio (h_1 / h_2) more than 2, increasing the thickness has a little effect on the results.

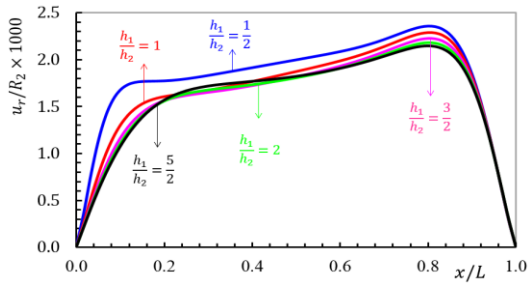

Fig.9
Distribution of non-dimensional radial displacement for different values of h_1 in the middle surface.

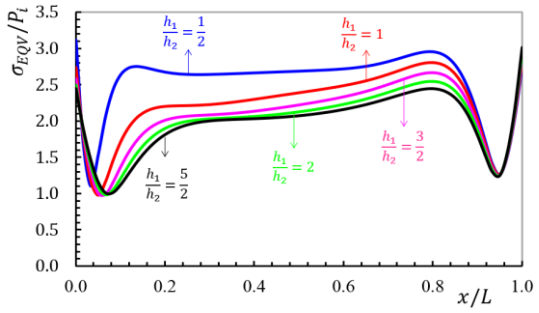

Fig.10
Distribution of non-dimensional von Mises stress for different values of h_1 in the middle surface.

Figs. 11 and 12 clearly reflect the influence of the different values of the thermal gradient in the dimensionless radial displacement and von Mises stress resultant at the middle layer of the conical shell with variable thickness. It is obvious that with increasing ΔT , radial displacement increases. But this statement satisfied for von Mises stress at points away from the boundaries.

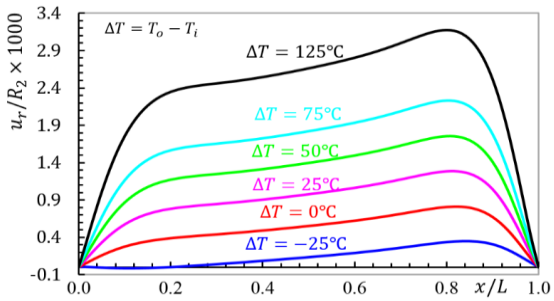

Fig.11
Effect of thermal gradient on the distribution of non-dimensional radial displacement.

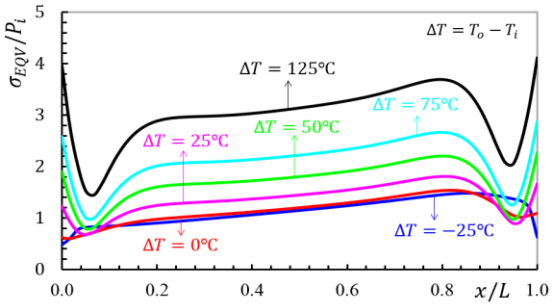

Fig.12
Effect of thermal gradient on the distribution of non-dimensional von Mises stress.

To examine the effect of loading type on the components of stress and radial displacement, nine different prescribed pressurized rotating conical shell are considered as shown in Figs. 13 and 14. The results of Figs. 13 and 14 can be summarized as follows:

1. The radial displacement of the cone under external pressure have negative value unlike the cone under internal pressure.
2. Radial displacement and von Mises stress increase as ω increases.
3. Conical shell subjected to pressure and centrifugal loading show same behavior as the cone under pressure loading, means that variation of the angular velocity has no considerable effect on the displacements and von Mises stress in the cone.
4. In the conical shell with variable thickness von Mises stress rises with decreases the value of external pressure.
5. The von Mises stress subjected to the thermal gradient is more than von Mises stress subjected to the external pressure loading.
6. The centrifugal force is less effective than the internal and external pressures and thermal gradient.

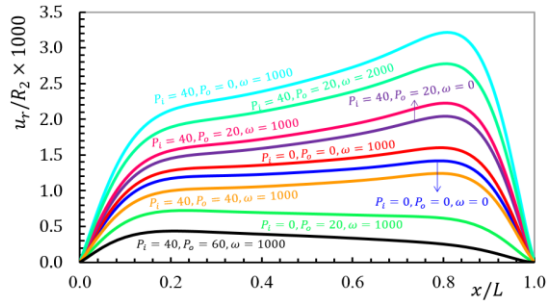

Fig.13
Effect of angular velocity and pressure profile on the distribution of non-dimensional radial displacement.

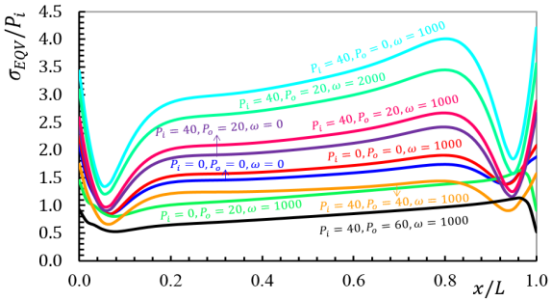

Fig.14
Effect of angular velocity and pressure profile on the distribution of non-dimensional von Mises stress.

5 CONCLUSIONS

This paper aims to develop analytical formulations and solutions for isotropic rotating thick-walled conical shells with variable thickness subjected to the internal pressure and external pressure and thermal gradient and using FSDT. The basic equations of truncated conical shells with variable thickness are derived and solved applying MLM for clamped-clamped boundary condition. The results performed for stresses and displacements are compared with

the solutions carried out through the FEM. Good agreement was found between the results. The effects of the centrifugal force, the geometry parameter such as inner radii and thickness variation of the cone and loading types, on the stresses and displacements are investigated.

In summary, the above results reveal that cones with variable thickness ($h_1 / h_2 > 1$) given have smaller equivalent stresses and radial displacement compared to cone with constant thickness. But the obtained results demonstrate that for the cones with variable thickness ($h_1 / h_2 > 2$), von Mises stress and radial displacement have not significant change. It is noted that the maximum value of von Mises stresses due to mechanical and thermal loading in cones with variable thickness under clamped-clamped condition occurs at near points from the boundaries. It is also noted that with increasing ΔT , radial displacement and von Mises stress increase at points away from the boundaries.

REFERENCES

[1] Eipakchi H. R., Khadem S. E., Rahimi G. H., 2008, Axisymmetric stress analysis of a thick conical shell with varying thickness under nonuniform internal pressure, *Journal of Engineering Mechanics* **134**(8): 601-610.

[2] Nejad M. Z., Jabbari M., Ghannad M., 2015, Elastic analysis of axially functionally graded rotating thick cylinder with variable thickness under non-uniform arbitrarily pressure loading, *International Journal of Engineering Science* **89**: 86-99.

[3] Ghasemi A. R., Kazemian A., Moradi M., 2014, Analytical and numerical investigation of FGM pressure vessel reinforced by laminated composite materials, *Journal of Solid Mechanics* **6**(1): 43-53.

[4] Nejad M. Z., Jabbari M., Ghannad M., 2015, Elastic analysis of rotating thick cylindrical pressure vessels under non-uniform pressure: linear and non-linear thickness, *Periodica Polytechnica Engineering, Mechanical Engineering* **59**(2): 65-73.

[5] Witt F.J., 1965, Thermal stress analysis of conical shells, *Nuclear Structure Engineering* **1**(5): 449-456.

[6] Panferov I. V., 1991, Stresses in a transversely isotropic conical elastic pipe of constant thickness under a thermal load, *Journal of Applied Mathematics and Mechanics* **56**(3): 410-415.

[7] Sundarasivarao B. S. K., Ganesan N. 1991, Deformation of varying thickness of conical shells subjected to axisymmetric loading with various end conditions, *Engineering Fracture Mechanics* **39**(6): 1003-1010.

[8] Jane K. C., Wu Y. H., 2004, A generalized thermoelasticity problem of multilayered conical shells, *International Journal of Solids Structures* **41**: 2205-2233.

[9] Vivio F., Vullo V., 2007, Elastic stress analysis of rotating converging conical disks subjected to thermal load and having variable density along the radius, *International Journal of Solids Structures* **44**: 7767-7784.

[10] Naj R., Boroujerdy M. B., Eslami M. R., 2008, Thermal and mechanical instability of functionally graded truncated conical shells, *Thin Walled Structures* **46**: 65-78.

[11] Eipakchi H. R., 2009, Errata for axisymmetric stress analysis of a thick conical shell with varying thickness under nonuniform internal pressure, *Journal of Engineering Mechanics* **135**(9): 1056-1056.

[12] Sladek J., Sladek V., Solek P., Wen P. H., Atluri A. N., 2008, Thermal analysis of reissner-mindlin shallow shells with FGM properties by the MLPG, *CMES: Computer Modelling in Engineering and Sciences* **30**(2): 77-97.

[13] Nejad M. Z., Rahimi G. H., Ghannad M., 2009, Set of field equations for thick shell of revolution made of functionally graded materials in curvilinear coordinate system, *Mechanika* **77**(3): 18-26.

[14] Ghannad M., Nejad M. Z., Rahimi G. H., 2009, Elastic solution of axisymmetric thick truncated conical shells based on first-order shear deformation theory, *Mechanika* **79**(5): 13-20.

[15] Eipakchi, H. R., 2010, Third-order shear deformation theory for stress analysis of a thick conical shell under pressure, *Journal of Mechanics of materials and structures* **5**(1): 1-17.

[16] Jabbari M., Meshkini M., Eslami M. R., 2011, Mechanical and thermal stresses in a FGPM hollow cylinder due to non-axisymmetric loads, *Journal of Solid Mechanics* **3**(1): 19-41.

[17] Ray S., Loukou A., Trimis D., 2012, Evaluation of heat conduction through truncated conical shells, *International Journal of Thermal Sciences* **57**: 183-191.

[18] Ghannad M., Gharooni H., 2012, Displacements and stresses in pressurized thick FGM cylinders with varying properties of power function based on HSDT, *Journal of Solid Mechanics* **4**(3): 237-251.

[19] Ghannad M., Nejad M. Z., Rahimi G. H., Sabouri H., 2012, Elastic analysis of pressurized thick truncated conical shells made of functionally graded materials, *Structural Engineering and Mechanics* **43**(1): 105-126.

[20] Nejad M. Z., Jabbari M., Ghannad M., 2014, A semi-analytical solution of thick truncated cones using matched asymptotic method and disk form multilayers, *Archive of Mechanical Engineering* **3**: 495-513.

[21] Nejad M. Z., Jabbari M., Ghannad M. 2014, Elastic analysis of rotating thick truncated conical shells subjected to uniform pressure using disk form multilayers, *ISRN Mechanical Engineering* **764837**: 1-10.

[22] Jabbari M., Meshkini M., 2014, Mechanical and thermal stresses in a FGPM hollow cylinder due to radially symmetric loads, *Encyclopedia of Thermal Stresses* 2938-2946.
[23] Nejad M. Z., Jabbari M., Ghannad M., 2015, Elastic analysis of FGM rotating thick truncated conical shells with axially-varying properties under non-uniform pressure loading, *Composite Structures* **122**: 561-569.
[24] Sofiyev A. H., Huseynov S. E., Ozyigit P., Isayev, F. G., 2015, The effect of mixed boundary conditions on the stability behavior of heterogeneous orthotropic truncated conical shells, *Meccanica* **50**: 2153-2166.
[25] Jabbari M., Nejad M. Z., Ghannad M., 2016, Thermoelastic analysis of rotating thick truncated conical shells subjected to non-uniform pressure, *Journal of Solid Mechanics* **8**(3): 481-466.
[26] Vlachoutsis S., 1992, Shear correction factors for plates and shells, *International Journal for Numerical Methods in Engineering* **33**: 1537-1552.
[27] Buchanan G. R., Yii C. B. Y., 2002, Effect of symmetrical boundary conditions on the vibration of thick hollow cylinders, *Applied Acoustics* **63**(5): 547-566.